This article has been accepted for publication in a future issue of this journal, but has not been fully edited. Content may change prior to final publication.
Citation information: DOI: 10.1109/TAC.2025.3637019, IEEE Transactions on Automatic Control

Chance-Constrained Dynamic Encoding-Based Control Over Noisy Communication Channels: An Active Bit-Flip-Error-Resistant Approach

Kaiqun Zhu, Zidong Wang, Derui Ding, Zhenning Li and Cheng-Zhong Xu

***Abstract*—This paper investigates the chance-constrained control problem for uncertain systems, with a focus on the distortion of signal transmission between the controller and the actuator caused by noisy and bandwidth-limited communication channels, and its impact on the system's control performance. Initially, a binary dynamic encoding mechanism (DEM) is employed to encode the system's amplitude-continuous signal into a finite-length binary string, aiming to mitigate the communication burden. In the DEM-based control scheme, a critical issue is that the control performance is seriously affected by the bit-flip error (BFE), which inevitably occurs during the transmission of binary data through a noisy channel. To address this problem, a novel active BFE-resistant controller is proposed to effectively accomplish the desired control task by thoroughly considering the dynamic coupling effects between the BFE and the DEM. Subsequently, a chance constraint index is jointly considered to ensure the safe operation of the uncertain system under a guaranteed probability bound. Sufficient conditions are established for the existence of the active BFE-resistant controller such that the mean-square boundedness and the chance constraint index are ensured simultaneously. Finally, the validity of the proposed algorithm is verified by a simulation study targeting the remote control problem for autonomous ground vehicles.**

***Index Terms*—Dynamic encoding mechanisms, bit-flip errors, mean-square boundedness, chance constraints, autonomous ground vehicles.**

I. Introduction

Over the past few decades, the rapid development of information and communication technology has facilitated the seamless integration of control systems with communication networks, which enables remote control and monitoring functionalities that were previously unattainable [14], [33]. This networked control paradigm has found widespread applications in various cutting-edge fields such as smart grids [15] and autonomous vehicles [25]. Despite recent progress, research on networked systems continues to face several persistent challenges. One of the most critical issues is the limited communication bandwidth, which may cause data distortion, reduce transmission quality, and ultimately degrade overall system performance [4], [6], [18], [22], [31], [36]. Consequently, it is essential to address the issues induced by limited bandwidth to ensure the desired performance of control systems.

In response to the limited bandwidth issue, data encoding technology has emerged as an ideal solution due to its benefits in data compression and encryption. By leveraging data encoding rule, large volumes of continuous data can be transformed into more manageable formats, thus optimizing the use of available bandwidth and enhancing data security during transmission. This technology is particularly advantageous in scenarios where high data throughput and secure communication are critical. Data encoding technology can be categorized into two distinct types: static encoding mechanisms [16], [17], [34] and dynamic encoding mechanisms (DEM) [11], [20], [38], depending on the employed quantization technique. The role of the encoding mechanism is to convert signals into finite-length binary strings, effectively reducing the amount of data to be transmitted and thereby decreasing the demand for bandwidth.

During the transmission of a binary string over a communication channel, various factors (e.g. electromagnetic radiations and channel noises) can lead to the flipping (or alteration) of one or more bits within the binary sequence [2], [10], [24]. This phenomenon is recognized as the *bit-flip error* (BFE) problem. Several results on BFE problems have been studied for systems under static encoding mechanisms, e.g., [19], [21], [28]. However, in the context of *dynamic encoding schemes*, the BFE issues have yet to be thoroughly investigated. The main difficulty lies in the dynamic coupling between the BFEs and DEMs, making it challenging to decouple BFEs from decoding errors, and thus preventing a direct analysis of the impact of BFEs on system performance. The primary objective of this article is to conduct an in-depth investigation into the BFE problem by focusing specifically on its implications within the context of DEMs.

The investigation of system constraints holds essential significance in practical engineering [3], [7], [12], [29]. The imposition of constraints on system variables is motivated by multifaceted factors, notably: 1) the inherent limitations pertaining to the operating ranges and capabilities of physical devices; 2) the indispensable imperative to guarantee the safety of system operation; and 3) the critical necessity to optimize system performance and avoid resource waste [1], [13], [27], [30]. Unfortunately, ensuring the satisfaction of constraints at all times becomes theoretically challenging when the underlying system is subject to stochastic noises arising from factors such as modeling errors and external disturbances.

For decades, the chance constraint, also known as a probabilistic constraint, has emerged as a powerful tool to handle uncertainties and enhance the performance and reliability of control systems. This method ensures that the probability of a specific event occurring remains above a pre-defined threshold [5], [23]. The chance constraint method provides a framework for performance optimization by balancing the performance index with the associated risks, which is of great significance for ensuring system reliability and enhancing the practicality of decision-making in real-world applications [8], [9], [26], [32], [35], [37]. Nevertheless, there has been a notable lack of research addressing the chance-constrained control problem

This work was supported in part by the National Natural Science Foundation of China under Grant 61933007, Grant 62403318, and Grant 52572354; in part by the Science and Technology Development Fund of Macao SAR under Grant 0123/2022/AFJ, Grant 0081/2022/A2, Grant 0122/2024/RIB2, Grant 0215/2024/AGJ, and Grant 001/2024/SKL; in part by the Science and Technology Planning Project of Guangdong under Grant 2025A0505010016; in part by the Royal Society of the UK; and in part by the Alexander von Humboldt Foundation of Germany. (*Corresponding author: Cheng-Zhong Xu.*)

Kaiqun Zhu and Zhenning Li are with the State Key Laboratory of Internet of Things for Smart City, University of Macau, Macau 999078, China. (Email: zkqun@163.com; zhenningli@um.edu.mo)

Zidong Wang is with the Department of Computer Science, Brunel University London, Uxbridge, Middlesex, UB8 3PH, United Kingdom. (Email: Zidong.Wang@brunel.ac.uk)

Derui Ding is with the Department of Control Science and Engineering, University of Shanghai for Science and Technology, Shanghai 200093, China. (Email: deruiding2010@usst.edu.cn)

Cheng-Zhong Xu is with the Department of Computer and Information Science, University of Macau, Macau 999078, China. (Email: czxu@um.edu.mo)

for systems affected by the BFE phenomenon. The limited attention given to this issue can be attributed to the rather complicated coupling effect between DEMs, BFEs, and chance constraints, which poses challenges in analyzing and optimizing system performance. Consequently, this serves as another motivation for our ongoing research.

This research endeavor is motivated by the need to explore the chance-constrained control issue under the influence of DEMs and BFEs. The critical challenges addressed in this paper include: 1) how to characterize the impact of DEMs and BFEs on system signals and analyze their effects on system performance? 2) how to design an apt controller structure to actively counteract the impact of BFE-affected signal distortion on system control performance? and 3) how to ensure that the anticipated performance of the system is met under the influence of BFE-affected signal distortion and stochastic noise?

Considering the challenges discussed above, this paper presents the following key contributions.

1) The dynamic characteristic of the decoding error is, for the first time, analyzed under the coupling influence of DEMs and BFEs, which provides the basis for the design of controller structure and analysis of control performance.
2) A novel BFE-resistant controller is proposed for systems under DEMs and chance constraints. By actively counteracting BFE-affected decoding errors, this controller effectively mitigates their impact on system control performance.
3) The chance constraint is transformed into a solvable deterministic matrix inequality under the influence of BFE-affected decoding errors, and sufficient conditions are derived for simultaneously achieving the mean-square boundedness and the chance constraint. Moreover, the controller parameters are determined by solving the chance-constrained optimization problem.

Notations: $\mathbb{E}[X]$ is the mathematical expectation of X; $\mathbf{Var}[X]$ means the variance of X; $\mathbf{Pr}\{Y\}$ denotes the probability of an event Y; $\mathrm{diag}\{\cdot\}$ is a block-diagonal matrix; $\mathrm{col}_n\{a_i\}$ represents $\begin{bmatrix} a_1 & a_2 & \cdots & a_n \end{bmatrix}^{\mathrm{T}}$; $\mathrm{diag}_n\{a_i\}$ denotes $\mathrm{diag}\{a_1, a_2, \ldots, a_n\}$; $\lfloor\cdot\rfloor$ denotes the function rounding downward to the nearest integer; $\lambda_{\max}(P)$ represents the maximum eigenvalue of a matrix P; $\mathrm{Tr}(P)$ means the trace of a matrix P; and functions $\mathbf{Q}[\cdot]$, $\mathbf{Enc}[\cdot]$, and $\mathbf{Dec}[\cdot]$ represent the uniform quantization, encoding, and decoding operations, respectively.

II. System Description

A. The System Model

Consider the following time-varying systems:

$$x_{t+1} = A_t x_t + B_t \vec{u}_t + w_t \tag{1}$$

where $x_t \in \mathbb{R}^{n_x}$ and $\vec{u}_t \in \mathbb{R}^{n_u}$ are the state variable and the control input; $w_t \in \mathbb{R}^{n_w}$ is the non-Gaussian stochastic noise with unknown distribution; and A_t, B_t, W_t, and $\bar{W}$ are known matrices. Here, $\mathbb{E}[w_t] = 0$, $\mathbf{Var}[w_t] = W_t > 0$, and $W_t \le \bar{W}$.

Ensuring the safe operation of real-world systems is of paramount importance. However, when stochastic noise is present, traditional deterministic constraint methods may fail to effectively handle such uncertainties. Therefore, it is essential to construct a framework that can quantify risk (i.e., constraint violation) and allow the system's constraints to be satisfied with a certain level of confidence, which is achieved by ensuring system performance within a specified probability threshold. This is the essence of chance constraints. Unlike traditional deterministic constraints, chance constraints are probabilistic in nature, requiring the constraints to be satisfied with a predetermined probability level, and the specific form is described as follows:

$$\mathbf{Pr}\{x_t^{\mathrm{T}} \Lambda_t^{-1} x_t \le 1\} \ge 1 - \epsilon_t \tag{2}$$

where $\Lambda_t > 0$ is the known matrix and $0 < \epsilon_t < 1$ is the maximum probability value of violating the state constraint.

B. The Binary Dynamic Encoding Mechanism

In networked control systems, the control input signal is transmitted to the actuator through a communication network with limited bandwidth. To alleviate the communication burden, a binary DEM is utilized in this paper. In the binary dynamic encoding scheme, the amplitude-continuous signal is processed through two steps: binary encoding and decoding. For simplicity purpose, we introduce the following notations:

$$\begin{aligned} &u_t \triangleq \mathrm{col}_{n_u}\{u_{i,t}\}, \quad \hat{u}_t \triangleq \mathrm{col}_{n_u}\{\hat{u}_{i,t}\}, \quad \acute{u}_t \triangleq \mathrm{col}_{n_u}\{\acute{u}_{i,t}\} \\ &\vec{u}_t \triangleq \mathrm{col}_{n_u}\{\vec{u}_{i,t}\}, \quad \chi_t \triangleq \mathrm{col}_{n_u}\{\chi_{i,t}\} \\ &\mathbf{a}_t \triangleq \mathrm{diag}_{n_u}\{\mathbf{a}_{i,t}\}, \quad \mathbf{b}_t \triangleq \mathrm{diag}_{n_u}\{\mathbf{b}_{i,t}\}. \end{aligned}$$

In the binary DEM, the uniform quantizer is utilized to convert the amplitude-continuous signal $u_{i,t}$ into the amplitude-discrete data:

$$\mathbf{Q}[u_{i,t}] = \left\lfloor \frac{u_{i,t}}{\rho} \right\rfloor \rho \tag{3}$$

where $\rho > 0$ is the resolution of the quantizer and $u_{i,t}$ means the i-th element of the original control input u_t.

Binary encoding step. The amplitude-continuous signal $u_{i,t}$ is first converted into the amplitude-discrete data $\hat{u}_{i,t}$ according to the following dynamic encoding rule:

$$\begin{cases} \chi_{i,t} = \mathbf{a}_{i,t}\chi_{i,t-1} + \mathbf{b}_{i,t}\hat{u}_{i,t} \\ \hat{u}_{i,t} = \mathbf{Q}\left[\frac{1}{\mathbf{b}_{i,t}}(u_{i,t} - \mathbf{a}_{i,t}\chi_{i,t-1})\right] \end{cases} \tag{4}$$

where $\chi_{i,t}$ is the dynamic variable, $\hat{u}_{i,t}$ is the encoded data, and $\mathbf{a}_{i,t}$ and $\mathbf{b}_{i,t}$ are known parameters.

Due to the fact that $\hat{u}_{i,t}$ represents the decimal data, it needs to be encoded into a binary string prior to communication network transmission. Specifically, we employ 1-bit for encoding the sign, $(\ell - \jmath - 1)$-bits for encoding the integer part, and $\jmath$-bits for encoding the fractional part. That is,

$$\underbrace{\beta_{i,t}^{[\ell]}}_{\pm\text{sign bit}} \underbrace{\beta_{i,t}^{[\ell-1]} \cdots \beta_{i,t}^{[\jmath+1]}}_{\text{integer bits}} . \underbrace{\beta_{i,t}^{[\jmath]} \cdots \beta_{i,t}^{[1]}}_{\text{fractional bits}} \tag{5}$$

where $\beta_{i,t}^{[j]} \in \{0, 1\}$ $(j = 1, 2, \ldots, \ell)$ denotes the binary value and ℓ is the number of total bits for encoding $\hat{u}_{i,t}$. According to (5), it is obvious that the encoding range is $[-2^{\ell-\jmath-1},\ 2^{\ell-\jmath-1})$ and the resolution is $2^{-\jmath}$ (also known as quantization interval).

As per the following binary encoding method, the decimal data can be represented using a binary string with finite bits:

$$\hat{u}_{i,t} \triangleq \mathbf{Enc}[\hat{u}_{i,t}] = -2^{\ell-\jmath-1}\beta_{i,t}^{[\ell]} + \sum_{j=1}^{\ell-1} 2^{j-\jmath-1}\beta_{i,t}^{[j]}. \tag{6}$$

Then, the finite-length binary string $\beta_{i,t}^{[\ell]}\beta_{i,t}^{[\ell-1]} \cdots \beta_{i,t}^{[1]}$ is transmitted to the decoder side through communication networks.

Decoding step. In the decoder, according to the decoding rule, the ideal decoder output is

$$\begin{aligned} \acute{u}_{i,t} &\triangleq \mathbf{Dec}\Big[\beta_{i,t}^{[\ell]}\beta_{i,t}^{[\ell-1]} \cdots \beta_{i,t}^{[1]}\Big] \\ &= \mathbf{a}_{i,t}\acute{u}_{i,t-1} + \mathbf{b}_{i,t}\Big(-2^{\ell-\jmath-1}\beta_{i,t}^{[\ell]} + \sum_{j=1}^{\ell-1} 2^{j-\jmath-1}\beta_{i,t}^{[j]}\Big) \\ &= \mathbf{a}_{i,t}\acute{u}_{i,t-1} + \mathbf{b}_{i,t}\hat{u}_{i,t} \end{aligned} \tag{7}$$

where $\acute{u}_{i,t}$ is the ideally decoded data (without the influence of BFEs). In addition, the initial condition satisfies $\acute{u}_{i,0} = \chi_{i,0}$.

It should be noted that, in network channels, the binary values may be *flipped* during transmission due to various reasons including electromagnetic radiation and channel noises. This phenomenon will be investigated in the following subsection.

C. The Bit-Flip Error Phenomenon

In network channels, the BFE problem may occur. That is, the binary value $\beta_{i,t}^{[j]}$ may be flipped into $1-\beta_{i,t}^{[j]}$. Under the influence of BFE, the actually received binary string at the decoder side is $\vec{\beta}_{i,t}^{[\ell]}\vec{\beta}_{i,t}^{[\ell-1]}\cdots\vec{\beta}_{i,t}^{[1]}$ where, for $j=1,2,\ldots,\ell$,

$$\vec{\beta}_{i,t}^{[j]} = \begin{cases} 1-\beta_{i,t}^{[j]}, & \text{the BFE occurs} \\ \beta_{i,t}^{[j]}, & \text{otherwise.} \end{cases}$$

The decoding process of the binary string under the influence of BFE is described as follows.

Decoding under BFEs. In the presence of BFEs, the actual output of the decoder is now given as

$$\begin{aligned} \vec{u}_{i,t} &\triangleq \mathbf{Dec}\Big[\vec{\beta}_{i,t}^{[\ell]}\vec{\beta}_{i,t}^{[\ell-1]}\cdots\vec{\beta}_{i,t}^{[1]}\Big] \\ &= \mathbf{a}_{i,t}\vec{u}_{i,t-1} + \mathbf{b}_{i,t}\Big(-2^{\ell-\jmath-1}\vec{\beta}_{i,t}^{[\ell]} + \sum_{j=1}^{\ell-1} 2^{j-\jmath-1}\vec{\beta}_{i,t}^{[j]}\Big) \\ &= \mathbf{a}_{i,t}\vec{u}_{i,t-1} + \mathbf{b}_{i,t}(\hat{u}_{i,t} + \xi_{i,t}) \end{aligned} \tag{8}$$

where $\vec{u}_{i,0} = \chi_{i,0}$, $\vec{u}_{i,t}$ is the i-th element of the actually decoded control input $\vec{u}_t$ (under the influence of BFEs), and $\xi_{i,t}$ denotes the BFE with

$$\xi_{i,t} \triangleq -2^{\ell-\jmath-1}(\vec{\beta}_{i,t}^{[\ell]} - \beta_{i,t}^{[\ell]}) + \sum_{j=1}^{\ell-1} 2^{j-\jmath-1}(\vec{\beta}_{i,t}^{[\ell]} - \beta_{i,t}^{[\ell]}).$$

By comparing the ideal decoding data $\acute{u}_{i,t}$ obtained from (7) with the BFE-influenced decoding data $\vec{u}_{i,t}$ from (8), it is evident that the coupling effect of the dynamic encoding-decoding rules and BFE complicates the analysis of decoding errors. Before analysis, let us first denote the BFE-affected decoding error as $e_t \triangleq \vec{u}_t - u_t$.

In the following, we will analyze the dynamic property of e_t. According to (4) and (8), we obtain

$$\begin{aligned} \vec{u}_t - \chi_t &= \mathbf{a}_t\vec{u}_{t-1} + \mathbf{b}_t(\hat{u}_t + \xi_t) - \mathbf{a}_t\chi_{t-1} - \mathbf{b}_t\hat{u}_t \\ &= \mathbf{a}_t(\vec{u}_{t-1} - \chi_{t-1}) + \mathbf{b}_t\xi_t. \end{aligned} \tag{9}$$

Then, as per (4) and (7), and employing the mathematical induction method [38], it is easy to show that

$$\chi_t = \acute{u}_t. \tag{10}$$

Based on (4) and (10), the BFE-affected decoding error e_t is derived as follows:

$$\begin{aligned} e_t &= \vec{u}_t - \chi_t + \chi_t - u_t \\ &= d_t + \acute{u}_t - u_t = d_t + \mathbf{b}_t e_{q,t} \end{aligned} \tag{11}$$

where $d_t \triangleq \vec{u}_t - \chi_t$, $d_t = \mathbf{a}_t d_{t-1} + \mathbf{b}_t\xi_t$, and

$$e_{q,t} \triangleq \mathbf{Q}\Big[\frac{1}{\mathbf{b}_t}(u_t - \mathbf{a}_t\chi_{t-1})\Big] - \frac{1}{\mathbf{b}_t}(u_t - \mathbf{a}_t\chi_{t-1}).$$

Through the above analysis, it is concluded that the BFE-affected decoding error (i.e., e_t) consists of two parts: data distortion caused by BFE (i.e., d_t) and data distortion caused by DEM (i.e., $e_{q,t}$). Note that the data distortion errors undergo a complex dynamic mapping within the DEM framework, resulting in decoding errors that exhibit intricate dynamic characteristics. This poses challenges for controller design and system performance analysis. Next, we will investigate the impact of this phenomenon on system control performance and propose an effective controller design method.

Remark 1: It is worth mentioning that, due to the underlying coupling between the DEM and the BFE, the dynamic property of the BFE-affected decoding error becomes extremely complicated, which brings further difficulties to the performance analysis of the system. According to (9)–(11), the BFE-affected decoding error satisfies

$$\begin{cases} e_t = d_t + \mathbf{b}_t e_{q,t} \\ d_t = \mathbf{a}_t d_{t-1} + \mathbf{b}_t\xi_t, \end{cases} \tag{12}$$

which indicates that e_t and d_t are unstable ($\lim_{t\to\infty} e_t = \infty$ and $\lim_{t\to\infty} d_t = \infty$) with $\lambda_{\max}(\mathbf{a}_t) > 1$. This complicated dynamic characterization may seriously deteriorate the system's performance. Therefore, there is a need to look for a controller design method to resist the undesirable result.

Remark 2: Note that, under limited bit-rate conditions, encoding mechanisms, particularly DEMs, play a crucial role in efficiently transmitting information required by the system. Existing literature has shown that, within the static encoding framework, the BFE-affected decoding error remains amplitude-bounded [19], [21]. However, under the DEM framework, the BFE-affected decoding error is prone to divergence, which presents further challenges for system analysis. It should be pointed out that this paper represents the first effort to analyze the BFE problem within the context of DEM.

D. The Active BFE-Resistant Controller

In this paper, based on the active counteraction method, the novel BFE-resistant controller is delineated in the following form:

$$u_t = F_t x_t - \hat{d}_t \tag{13}$$

where F_t is the controller parameter to be calculated and $\hat{d}_t$ is the variable to be determined for resisting the influence of BFE-affected decoding error.

By considering (1) and (11), the variable $\hat{d}_t$ is obtained by

$$\begin{cases} \eta_t = (\mathbf{a}_t + L_t B_{t-1})\hat{d}_{t-1} + L_t(A_{t-1}x_{t-1} + B_{t-1}u_{t-1}) \\ \hat{d}_t = \eta_t - L_t x_t \end{cases} \tag{14}$$

where $\eta_t \in \mathbb{R}^{n_\eta}$ is the dynamic variable and L_t is the parameter matrix to be obtained. By denoting $\mu_t \triangleq d_t - \hat{d}_t$, one obtains

$$\mu_t = (\mathbf{a}_t + L_t B_{t-1})\mu_{t-1} + \vec{\xi}_{t-1} + L_t w_{t-1} \tag{15}$$

where $\vec{\xi}_{t-1} \triangleq L_t B_{t-1}\mathbf{b}_{t-1}e_{q,t-1} + \mathbf{b}_t\xi_t$.

Letting $z_t \triangleq \begin{bmatrix} x_t^{\mathrm{T}} & \mu_t^{\mathrm{T}} \end{bmatrix}^{\mathrm{T}}$, the closed-loop system is obtained as follows:

$$z_{t+1} = \mathscr{A}_t z_t + \varpi_t \tag{16}$$

where

$$\mathscr{A}_t \triangleq \begin{bmatrix} A_t + B_t F_t & B_t \\ 0 & \mathbf{a}_{t+1} + L_{t+1}B_t \end{bmatrix},\ \varpi_t \triangleq \begin{bmatrix} B_t\mathbf{b}_t e_{q,t} + w_t \\ \vec{\xi}_t + L_{t+1}w_t \end{bmatrix}.$$

The aim of this paper is to derive the gain matrices F_t and L_t of an active BFE-resistant controller for systems subject to chance constraints and BFEs, so as to guarantee that the system is mean-square bounded and that the chance constraint holds.

III. Main Results

In this section, the performance of the mean-square boundedness and the chance constraint will be analyzed and the BFE-resistant controller will be calculated by solving the chance-constrained optimization problem.

A. Analysis of the Mean-Square Boundedness

The following theorem addresses the impact of stochastic noise and BFEs on system performance and provides a sufficient condition to ensure the system's mean-square boundedness.

Theorem 1: Let matrices F_t and L_t be given. For system (16), if there exist positive scalars $\hbar$, λ, ϕ_t and positive-definite matrix P_t such that

$$\vec{\mathscr{A}}_t^{\mathrm{T}}\mathscr{P}_{t+1}^{-1}\vec{\mathscr{A}}_t-\Upsilon_{1,t}\leq 0 \tag{17}$$

$$\mathscr{D}_t^{\mathrm{T}}\mathscr{P}_{t+1}^{-1}\mathscr{D}_t-\lambda I\leq 0 \tag{18}$$

$$\vec{\mathscr{A}}_t^{\mathrm{T}}\vec{\mathscr{A}}_t-\Upsilon_{2,t}\leq 0 \tag{19}$$

$$\mathscr{D}_t^{\mathrm{T}}\mathscr{D}_t-(\phi_t-\lambda)I\leq 0 \tag{20}$$

hold with the initial condition $z_0^{\mathrm{T}}P_0z_0\leq\hbar^{-1}\lambda\Gamma$, where

$$\begin{aligned}
&\vec{\mathscr{A}}_t\triangleq\begin{bmatrix}\mathscr{A}_t & \mathscr{D}_t & I\end{bmatrix},\quad \mathscr{D}_t\triangleq\begin{bmatrix}I^{\mathrm{T}} & L_{t+1}^{\mathrm{T}}\end{bmatrix}^{\mathrm{T}}\\
&\Upsilon_{1,t}\triangleq\mathrm{diag}\{(1-\hbar)P_t,\lambda I,\lambda I\},\quad \mathscr{P}_t\triangleq P_t^{-1}\\
&\Upsilon_{2,t}\triangleq\mathrm{diag}\{\hbar P_t,(\phi_t-\lambda)I,(\phi_t-\lambda)I\}\\
&\Gamma\triangleq\mathrm{Tr}(\bar{W})+\lambda_{\max}(\mathbf{b}_t^{\mathrm{T}}B_t^{\mathrm{T}}B_t\mathbf{b}_t)n_u2^{-2\jmath}\\
&\quad+\lambda_{\max}(\mathbf{b}_{t+1}^{\mathrm{T}}\mathbf{b}_{t+1})n_u2^{2\ell-2\jmath},
\end{aligned}$$

then the system is mean-square bounded over the finite-horizon.

Proof: Define the following function:

$$\begin{aligned}
\mathscr{H}_{t+1}\triangleq{}& z_{t+1}^{\mathrm{T}}P_{t+1}z_{t+1}-(1-\hbar)z_t^{\mathrm{T}}P_tz_t-\lambda w_t^{\mathrm{T}}w_t\\
&-\lambda v_t^{\mathrm{T}}v_t-\lambda\zeta_t^{\mathrm{T}}\zeta_t
\end{aligned}\tag{21}$$

where $v_t\triangleq B_t\mathbf{b}_te_{q,t}$ and $\zeta_t\triangleq\begin{bmatrix}0^{\mathrm{T}} & (\mathbf{b}_{t+1}\xi_{t+1})^{\mathrm{T}}\end{bmatrix}^{\mathrm{T}}$. Then, by substituting (16) into (21), calculating the mathematical expectation of (21), and performing some algebraic manipulations, we obtain

$$\begin{aligned}
\mathbb{E}[\mathscr{H}_{t+1}]={}&\vec{z}_t^{\mathrm{T}}\Big(\vec{\mathscr{A}}_t^{\mathrm{T}}P_{t+1}\vec{\mathscr{A}}_t-\mathrm{diag}\{(1-\hbar)P_t,\lambda I,\lambda I\}\Big)\vec{z}_t\\
&+\mathrm{Tr}(\mathscr{D}_t^{\mathrm{T}}P_{t+1}\mathscr{D}_tW_t-\lambda W_t)
\end{aligned}\tag{22}$$

where $\vec{z}_t\triangleq\begin{bmatrix}z_t^{\mathrm{T}} & v_t^{\mathrm{T}} & \zeta_t^{\mathrm{T}}\end{bmatrix}^{\mathrm{T}}$.

As per (17), (18) and (22), it is easy to infer $\mathbb{E}[\mathscr{H}_{t+1}]\leq 0$, which further yields

$$\mathbb{E}[V_{t+1}-(1-\hbar)V_t]\leq\lambda\mathrm{Tr}(W_t)+\lambda v_t^{\mathrm{T}}v_t+\lambda\zeta_t^{\mathrm{T}}\zeta_t \tag{23}$$

with $V_t\triangleq z_t^{\mathrm{T}}P_tz_t$.

Next, we aim to prove that $\mathbb{E}[V_t]\leq\hbar^{-1}\lambda\Gamma$ is always satisfied by using mathematical induction method, where $\Gamma\triangleq\mathrm{Tr}(\bar{W})+\lambda_{\max}(\mathbf{b}_t^{\mathrm{T}}B_t^{\mathrm{T}}B_t\mathbf{b}_t)n_u2^{-2\jmath}+\lambda_{\max}(\mathbf{b}_{t+1}^{\mathrm{T}}\mathbf{b}_{t+1})n_u2^{2\ell-2\jmath}$. In the initial step, it is obvious that $\mathbb{E}[V_0]\leq\hbar^{-1}\lambda\Gamma$ is fulfilled. In the inductive step, assume that $\mathbb{E}[V_t]\leq\hbar^{-1}\lambda\Gamma$. Then, combining (23), we have $\mathbb{E}[V_{t+1}]\leq\mathbb{E}[(1-\hbar)V_t]+\lambda\Gamma\leq(1-\hbar)\hbar^{-1}\lambda\Gamma+\lambda\Gamma=\hbar^{-1}\lambda\Gamma$. Accordingly, the condition $\mathbb{E}[V_t]\leq\hbar^{-1}\lambda\Gamma$ is always satisfied.

To analyze the mean-square boundedness of the system, we further define the following function:

$$\begin{aligned}
\mathscr{J}_{t+1}\triangleq{}& z_{t+1}^{\mathrm{T}}z_{t+1}-\hbar V_t-(\phi_t-\lambda)w_t^{\mathrm{T}}w_t\\
&-(\phi_t-\lambda)v_t^{\mathrm{T}}v_t-(\phi_t-\lambda)\zeta_t^{\mathrm{T}}\zeta_t.
\end{aligned}\tag{24}$$

Then, taking the mathematical expectation of (24), we obtain

$$\begin{aligned}
\mathbb{E}[\mathscr{J}_{t+1}]={}&\vec{z}_t^{\mathrm{T}}\Big(\vec{\mathscr{A}}_t^{\mathrm{T}}\vec{\mathscr{A}}_t-\mathrm{diag}\{\hbar P_t,(\phi_t-\lambda)I,(\phi_t-\lambda)I\}\Big)\vec{z}_t\\
&+\mathrm{Tr}(\mathscr{D}_t^{\mathrm{T}}\mathscr{D}_tW_t)-(\phi_t-\lambda)\mathrm{Tr}(W_t).
\end{aligned}\tag{25}$$

In line with (19), (20) and (25), it is easy to have

$$\mathbb{E}[\mathscr{J}_{t+1}]\leq 0. \tag{26}$$

By further combining (26) with $\mathbb{E}[V_t]\leq\hbar^{-1}\lambda\Gamma$, one has

$$\begin{aligned}
\mathbb{E}[z_{t+1}^{\mathrm{T}}z_{t+1}]&\leq\hbar\mathbb{E}[V_t]+(\phi_t-\lambda)(\mathrm{Tr}(W_t)+v_t^{\mathrm{T}}v_t+\zeta_t^{\mathrm{T}}\zeta_t)\\
&\leq\hbar\hbar^{-1}\lambda\Gamma+(\phi_t-\lambda)\Gamma=\phi_t\Gamma,
\end{aligned}\tag{27}$$

which means that system (16) is indeed mean-square bounded. Thus, the proof is now complete. ∎

Remark 3: From Theorem 1, it is obvious that the active BFE-resistant controller proposed in this paper is capable of effectively ensuring the system's performance. In the following, it will be shown that the system (1) may become unstable when a traditional state feedback controller is used, i.e.,

$$u_t=F_tx_t, \tag{28}$$

to stabilize the system. By substituting (28) into system (1), we obtain the closed-loop system of the following form:

$$x_{t+1}=(A_t+B_tF_t)x_t+B_t(d_t+\mathbf{b}_te_{q,t})+w_t. \tag{29}$$

Then, by utilizing a similar method as given in Theorem 1, it is straightforward to obtain that

$$\begin{aligned}
\mathbb{E}[x_{t+1}^{\mathrm{T}}x_{t+1}]\leq{}&\phi_{x,t}(\mathrm{Tr}(W_t)+(B_td_t)^{\mathrm{T}}(B_td_t)\\
&+(B_t\mathbf{b}_te_{q,t})^{\mathrm{T}}(B_t\mathbf{b}_te_{q,t}))
\end{aligned}\tag{30}$$

with $\phi_{x,t}$ being a positive scalar. From (30), it is clear that the upper bound of $\mathbb{E}[x_{t+1}^{\mathrm{T}}x_{t+1}]$ is related to the variable d_t. According to (12), it is known that $(B_td_t)^{\mathrm{T}}(B_td_t)$ is divergent if $\lambda_{\max}(\mathbf{a}_t)>1$. Thus, the traditional state feedback controller (28) cannot guarantee the desired control performance.

B. Analysis of the Chance Constraint

In what follows, a theorem is given to guarantee that the chance constraint (2) is met.

Lemma 1: Let the matrix L_t be given. For system (15), if there exist positive scalars h, κ, ψ_t, and positive-definite matrix Q_t such that the following conditions hold:

$$\Phi_t^{\mathrm{T}}\mathscr{Q}_{t+1}^{-1}\Phi_t-\Upsilon_{3,t}\leq 0 \tag{31}$$

$$\Phi_t^{\mathrm{T}}\Phi_t-\Upsilon_{4,t}\leq 0 \tag{32}$$

$$(L_{t+1}B_t\mathbf{b}_t)^{\mathrm{T}}(L_{t+1}B_t\mathbf{b}_t)-\gamma_tI\leq 0 \tag{33}$$

where

$$\begin{aligned}
&\Phi_t\triangleq\begin{bmatrix}\mathbf{a}_{t+1}+L_{t+1}B_t\mathbf{a}_t & I & L_{t+1}\end{bmatrix},\quad \mathscr{Q}_t\triangleq Q_t^{-1}\\
&\Upsilon_{3,t}\triangleq\mathrm{diag}\{(1-h)Q_t,\kappa I\},\quad \bar{w}\triangleq\max\|w_t\|^2\\
&\Upsilon_{4,t}\triangleq\mathrm{diag}\{hQ_t,(\psi_t-\kappa)I\},
\end{aligned}$$

then the system is bounded and, furthermore, we have $\mu_t^{\mathrm{T}}\mu_t\leq\vec{\psi}_t$ with $\vec{\psi}_t\triangleq\psi_t\big(\bar{w}+\lambda_{\max}(\mathbf{b}_t^{\mathrm{T}}B_t^{\mathrm{T}}B_t\mathbf{b}_t)n_u2^{-2\jmath}+\lambda_{\max}(\mathbf{b}_{t+1}^{\mathrm{T}}\mathbf{b}_{t+1})n_u2^{2\ell-2\jmath}\big)$.

Proof: The proof of this lemma is similar to that of Theorem 1, and is thus omitted here. ∎

Theorem 2: Let the matrix F_t be given. For system (1), if there exist a positive scalar σ_t such that

$$\frac{W_t}{\sigma_t}+\frac{\Xi_t\Xi_t^{\mathrm{T}}}{(1-\sigma_t\frac{n_x}{\epsilon_{t+1}})\varrho_t^{-1}}-\Lambda_{t+1}\leq 0 \tag{34}$$

where

$$\begin{aligned}
&\Xi_t\triangleq\begin{bmatrix}A_t+B_tF_t & B_t\mathbf{a}_t & B_t\mathbf{b}_t\end{bmatrix}\\
&\varrho_t\triangleq x_t^{\mathrm{T}}x_t+\vec{\psi}_t+2n_u(2^{-2\jmath}+2^{2\ell-2\jmath}),
\end{aligned}$$

then the chance constraint (2) is fulfilled.

Proof: First, combining with (11) and (13), system (1) can be rewritten as

$$x_{t+1}=\Xi_t\vec{x}_t+w_t \tag{35}$$

where $\vec{x}_t\triangleq\begin{bmatrix}x_t^{\mathrm{T}} & \mu_t^{\mathrm{T}} & \xi_t^{\mathrm{T}}\end{bmatrix}^{\mathrm{T}}$.

Next, we will investigate the deterministic transformation method for chance constraints. By incorporating the chance constraint index with the statistical properties of the stochastic noise, we construct the following form of the function:

$$\mathscr{G}_{t+1} \triangleq 1 - x_{t+1}^{\mathrm{T}}\Lambda_{t+1}^{-1}x_{t+1} - \sigma_t\Big(\frac{n_x}{\epsilon_{t+1}} - w_t^{\mathrm{T}}W_t^{-1}w_t\Big). \tag{36}$$

Then, by applying the completing-the-square technique with respect to x_{t+1}, the function (36) can be rearranged as

$$\begin{aligned}\mathscr{G}_{t+1} = {} & (x_{t+1} - x_{t+1}^{\star})^{\mathrm{T}}\Pi_{t+1}(x_{t+1} - x_{t+1}^{\star}) \\ & - \acute{x}_{t+1}^{\mathrm{T}}\Pi_{t+1}^{-1}\acute{x}_{t+1} + \vartheta_{t+1}\end{aligned} \tag{37}$$

where $x_{t+1}^{\star} \triangleq \Pi_{t+1}^{-1}\acute{x}_{t+1}$, $\Pi_{t+1} \triangleq \sigma_t W_t^{-1} - \Lambda_{t+1}^{-1}$, $\acute{x}_{t+1} \triangleq \sigma_t W_t^{-1}\bar{x}_{t+1}$, $\bar{x}_{t+1} \triangleq \Xi_t\vec{x}_t$, and $\vartheta_{t+1} \triangleq 1 - \sigma_t\frac{n_x}{\epsilon_{t+1}} + \sigma_t\bar{x}_{t+1}^{\mathrm{T}}W_t^{-1}\bar{x}_{t+1}$.

With the aid of the Matrix Inverse Lemma, it is calculated that

$$\Pi_{t+1}^{-1} = \sigma_t^{-1}W_t + \sigma_t^{-1}W_t\vec{\Lambda}_{t+1}^{-1}\sigma_t^{-1}W_t \tag{38}$$

where $\vec{\Lambda}_{t+1} \triangleq \Lambda_{t+1} - \sigma_t^{-1}W_t$.

By substituting (38) into $-\acute{x}_{t+1}^{\mathrm{T}}\Pi_{t+1}^{-1}\acute{x}_{t+1} + \vartheta_{t+1}$ in (37) and simplifying, we obtain:

$$-\acute{x}_{t+1}^{\mathrm{T}}\Pi_{t+1}^{-1}\acute{x}_{t+1} + \vartheta_{t+1} = 1 - \sigma_t\frac{n_x}{\epsilon_{t+1}} - \bar{x}_{t+1}^{\mathrm{T}}\vec{\Lambda}_{t+1}^{-1}\bar{x}_{t+1}. \tag{39}$$

Then, by substituting (39) into (37), we have

$$\begin{aligned}\mathscr{G}_{t+1} = {} & (x_{t+1} - x_{t+1}^{\star})^{\mathrm{T}}\Pi_{t+1}(x_{t+1} - x_{t+1}^{\star}) \\ & + 1 - \sigma_t\frac{n_x}{\epsilon_{t+1}} - \bar{x}_{t+1}^{\mathrm{T}}\vec{\Lambda}_{t+1}^{-1}\bar{x}_{t+1}.\end{aligned} \tag{40}$$

By utilizing Lemma 1 and combining with (35), one has

$$\vec{x}_t^{\mathrm{T}}\vec{x}_t = x_t^{\mathrm{T}}x_t + \mu_t^{\mathrm{T}}\mu_t + \xi_t^{\mathrm{T}}\xi_t \le \varrho_t \tag{41}$$

where $\varrho_t \triangleq x_t^{\mathrm{T}}x_t + \vec{\psi}_t + 2n_u(2^{-2\jmath} + 2^{2\ell-2\jmath})$. Then, according to (41), it is readily seen that $\vec{x}_t\vec{x}_t^{\mathrm{T}} \le \varrho_t I$, which further results in

$$\bar{x}_{t+1}\bar{x}_{t+1}^{\mathrm{T}} = \Xi_t\vec{x}_t\vec{x}_t^{\mathrm{T}}\Xi_t^{\mathrm{T}} \le \varrho_t\Xi_t\Xi_t^{\mathrm{T}}. \tag{42}$$

Combining (34) and (42) together, it is obvious that the following inequality holds:

$$-\Lambda_{t+1} + \frac{W_t}{\sigma_t} + \frac{\bar{x}_{t+1}\bar{x}_{t+1}^{\mathrm{T}}}{1 - \sigma_t\frac{n_x}{\epsilon_{t+1}}} \le 0. \tag{43}$$

Applying Schur Complement Lemma to (43), we can readily obtain

$$\begin{bmatrix} 1 - \sigma_t\frac{n_x}{\epsilon_{t+1}} & * \\ \bar{x}_{t+1} & \Lambda_{t+1} - \sigma_t^{-1}W_t \end{bmatrix} \ge 0. \tag{44}$$

Utilizing Schur Complement Lemma again, it follows from (44) that

$$1 - \sigma_t\frac{n_x}{\epsilon_{t+1}} - \bar{x}_{t+1}^{\mathrm{T}}\vec{\Lambda}_{t+1}^{-1}\bar{x}_{t+1} \ge 0 \tag{45}$$

where $\vec{\Lambda}_{t+1} \triangleq \Lambda_{t+1} - \sigma_t^{-1}W_t$, which, in conjunction with (40), implies that

$$\mathscr{G}_{t+1} \ge 0. \tag{46}$$

Using the S-procedure Lemma, it follows from (36) and (46) that

$$\frac{n_x}{\epsilon_{t+1}} - w_t^{\mathrm{T}}W_t^{-1}w_t \ge 0 \Longrightarrow 1 - x_{t+1}^{\mathrm{T}}\Lambda_{t+1}^{-1}x_{t+1} \ge 0. \tag{47}$$

From (47), it is straightforward to show that the following inequality is satisfied:

$$\mathbf{Pr}\Big\{x_{t+1}^{\mathrm{T}}\Lambda_{t+1}^{-1}x_{t+1} \le 1\Big\} \ge \mathbf{Pr}\Big\{w_t^{\mathrm{T}}W_t^{-1}w_t \le \frac{n_x}{\epsilon_{t+1}}\Big\}. \tag{48}$$

Then, by employing the Chebyshev inequality, it is clearly that the following inequality holds:

$$\mathbf{Pr}\Big\{w_t^{\mathrm{T}}W_t^{-1}w_t \le \frac{n_x}{\epsilon_{t+1}}\Big\} \ge 1 - \epsilon_{t+1}, \tag{49}$$

which, in combination with (47)–(48), results in

$$\mathbf{Pr}\Big\{x_{t+1}^{\mathrm{T}}\Lambda_{t+1}^{-1}x_{t+1} \le 1\Big\} \ge 1 - \epsilon_{t+1}. \tag{50}$$

Therefore, the proof is complete. ■

C. Optimization of Active BFE-Resistant Controller Parameters

In the following, the active BFE-resistant controller is obtained by calculating the chance-constrained optimization problem to achieve the desired performance indices.

Theorem 3: For system (16), the mean-square boundedness and the chance constraint are guaranteed if there exist matrices F_t and L_t such that the following optimization problem

$$\mathbf{OP}: \min_{F_t, L_t, \phi_t, \psi_t} \ \tau_t + \vec{\psi}_t \quad \text{s.t.} \begin{cases} z_{t+1} = \mathscr{A}_t z_t + \varpi_t \\ \Omega_{\imath,t} \le 0, \quad \imath = 1, 2, \ldots, 8 \end{cases} \tag{51}$$

is feasible, where

$$\begin{aligned}
\tau_t &\triangleq \phi_t\Big(\mathrm{Tr}(W_t) + \lambda_{\max}(\mathbf{b}_t^{\mathrm{T}}B_t^{\mathrm{T}}B_t\mathbf{b}_t)n_u2^{-2\jmath} \\
&\quad + \lambda_{\max}(\mathbf{b}_{t+1}^{\mathrm{T}}\mathbf{b}_{t+1})n_u2^{2\ell-2\jmath}\Big) \\
\Omega_{1,t} &\triangleq \begin{bmatrix} -\Upsilon_{1,t} & * \\ \vec{\mathscr{A}}_t & -\mathscr{P}_{t+1} \end{bmatrix}, \quad \Omega_{2,t} \triangleq \begin{bmatrix} -\lambda I & * \\ \mathscr{D}_t & -\mathscr{P}_{t+1} \end{bmatrix} \\
\Omega_{3,t} &\triangleq \begin{bmatrix} -\Upsilon_{2,t} & * \\ \vec{\mathscr{A}}_t & -I \end{bmatrix}, \quad \Omega_{4,t} \triangleq \begin{bmatrix} -(\phi_t - \lambda)I & * \\ \mathscr{D}_t & -I \end{bmatrix} \\
\Omega_{5,t} &\triangleq \begin{bmatrix} -\Upsilon_{3,t} & * \\ \Phi_t & -\mathscr{Q}_{t+1} \end{bmatrix}, \quad \Omega_{6,t} \triangleq \begin{bmatrix} -\Upsilon_{4,t} & * \\ \Phi_t & -I \end{bmatrix} \\
\Omega_{7,t} &\triangleq \begin{bmatrix} -\gamma_t & * \\ L_{t+1}B_t\mathbf{b}_t & -I \end{bmatrix}, \quad \vec{\varrho}_t \triangleq \Big(1 - \sigma_t\frac{n_x}{\epsilon_{t+1}}\Big)\varrho_t^{-1} \\
\Omega_{8,t} &\triangleq \begin{bmatrix} -\Lambda_{t+1} & * & * \\ \Xi_t^{\mathrm{T}} & -\vec{\varrho}_t I & * \\ W_t^{\frac{1}{2}} & 0 & -\sigma_t I \end{bmatrix}.
\end{aligned}$$

Proof: The proof is straightforward and therefore omitted for the conciseness. ■

Remark 4: In this article, we have embarked on a comprehensive exploration of chance-constrained control issue for uncertain systems influenced by BFEs and stochastic noises. Compared with the state-of-the-art results (see [19], [21], [26], [37]), the main innovations and contributions of this paper are summarized as follows: 1) *the studied control problem is new* as it thoroughly analyzes the chance-constrained control problem under the coupled influence of BFEs, DEMs, and stochastic noises. This paper investigates the dynamic characteristics of BFE-affected decoding errors and addresses their impact on system control performance; and 2) *the designed active BFE-resistant controller is novel* as it effectively mitigates the degradation of system performance caused by BFEs, ensuring mean-square boundedness and adherence to the chance constraint.

IV. Illustrative Example

In this section, the tracking control problem for autonomous ground vehicles (AGVs) is utilized to demonstrate the usefulness of the proposed control algorithm.

A. Parameter Setups

The variables associated with the AGV are defined as follows: v_l and v_r denote the velocities of the left and right wheels, respectively; $\flat$ represents the wheelbase; v is the linear velocity of the AGV, given by $v = \frac{v_l + v_r}{2}$; w_a denotes the angular velocity, computed as

$w_a = \frac{v_r - v_l}{b}$; θ denotes the orientation (heading angle); and (p_x, p_y) represents the planar position of the AGV.

The kinematics of the AGV is modeled as follows:

$$\underbrace{\begin{bmatrix}\dot{p}_x\\ \dot{p}_y\\ \dot{\theta}\end{bmatrix}}_{\dot{x}} = \begin{bmatrix}\cos(\theta) & 0\\ \sin(\theta) & 0\\ 0 & 1\end{bmatrix} \underbrace{\begin{bmatrix}v\\ w_a\end{bmatrix}}_{u} \tag{52}$$

where x denotes the state vector and u is the control input.

The model of the reference trajectory is given as

$$\underbrace{\begin{bmatrix}\dot{r}_x\\ \dot{r}_y\\ \dot{\theta}_r\end{bmatrix}}_{\dot{r}} = \begin{bmatrix}\cos(\theta_r) & 0\\ \sin(\theta_r) & 0\\ 0 & 1\end{bmatrix} \underbrace{\begin{bmatrix}v_r\\ w_r\end{bmatrix}}_{u_r} \tag{53}$$

where r and u_r are, respectively, the state vector and the control input of the reference trajectory.

Letting $\phi \triangleq \begin{bmatrix}\phi_x^{\mathrm{T}} & \phi_y^{\mathrm{T}} & \phi_\theta^{\mathrm{T}}\end{bmatrix}^{\mathrm{T}}$ be the tracking error, one has

$$\phi = \begin{bmatrix}\cos(\theta) & \sin(\theta) & 0\\ -\sin(\theta) & \cos(\theta) & 0\\ 0 & 0 & 1\end{bmatrix} \begin{bmatrix}p_x - r_x\\ p_y - r_y\\ \theta - \theta_r\end{bmatrix}. \tag{54}$$

Then, according to (52)–(54), the error state dynamic model (with the time-varying linear and angular velocities) are derived as follows:

$$\dot{\phi}_t = \underbrace{\begin{bmatrix}0 & w_{r,t} & 0\\ -w_{r,t} & 0 & v_{r,t}\\ 0 & 0 & 0\end{bmatrix}}_{\mathbf{A}_t} \phi_t + \underbrace{\begin{bmatrix}1 & 0\\ 0 & 0\\ 0 & 1\end{bmatrix}}_{\mathbf{B}} u_t \tag{55}$$

where $v_{r,t}$ and $w_{r,t}$ are, respectively, the linear and angular velocities of the reference trajectory, and $u_t \triangleq \begin{bmatrix}v_{r,t}\cos(\phi_{\theta,t}) - v_t\\ w_{r,t} - w_t\end{bmatrix}$. In order to implement the designed controller on the digital platform, we discretize system (55) by the zero-order hold sampling method.

The eight-shaped reference trajectory is considered in this section, which is defined as $r_x = 3\sin(t)$ and $r_y = 2\sin(2t)$. The time-varying linear and angular velocities are

$$\begin{cases} v_t = \sqrt{(3\cos(t))^2 + (4\cos(2t))^2)} \\ w_{a,t} = \frac{1}{v_t}(3\cos(t) + 4\cos(2t)). \end{cases}$$

In addition, the values of the other variables are set as follows: $\mathbf{a}_t = 1.1I$, $\mathbf{b}_t = 2I$, $W_t = 0.1I$, $\epsilon_t = 0.05$, $\ell = 8$, and

$$\Lambda_t = \begin{cases} 3(1.3 - 0.2t)^2 I, & 0 \le t \le 3 \\ 3(1 - 0.1t)^2 I, & 4 \le t \le 8 \\ 0.2^2 I, & \text{others.} \end{cases}$$

B. Analysis of Experimental Results

A series of comparative experiments are conducted to comprehensively evaluate the effectiveness of the proposed control algorithm. The experiments include: comparison between open-loop and closed-loop control performance; comparison between the proposed control method and conventional state feedback control algorithm; evaluation of different approaches for handling chance constraints; comparison between dynamic and static encoding mechanisms; and performance comparison under various levels of BFEs. The detailed simulation results are presented as follows.

1) Open-loop and closed-loop control: In this subsection, we first compare the performance of open-loop and closed-loop control performance. Fig. 1 illustrates the reference path and the tracking path of the AGV with and without the control input, respectively. It is clear that the open-loop control system cannot ensure the desired tracking performance, while the control input computed in this paper is capable of stabilizing the tracking error system.

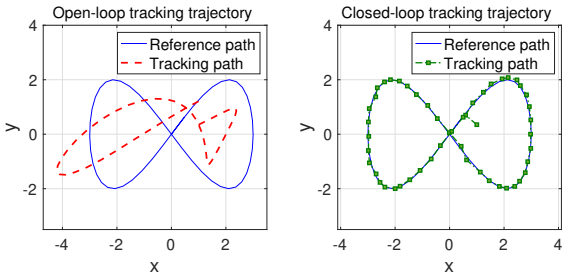

Fig. 1: Trajectory tracking performance under open-loop control (left) and closed-loop control (right) algorithms.

2) The proposed BFE-resistant controller and the traditional state feedback controller: Next, we evaluate the control performance under the influence of BFEs. In this simulation, the BFE problem occurs at integer-bit positions of the transmitted signal during the time interval $5 \le t \le 6$. Fig. 2 illustrates the trajectory tracking performance of the AGV under the BFE-resistant control algorithm proposed in this paper and the conventional state feedback control approach, respectively. As shown in the figure, after the occurrence of BFEs, the proposed BFE-resistant control strategy is capable of effectively stabilizing the system and maintaining satisfactory tracking performance, whereas the classical state feedback control algorithm fails to ensure that the AGV follows the reference trajectory.

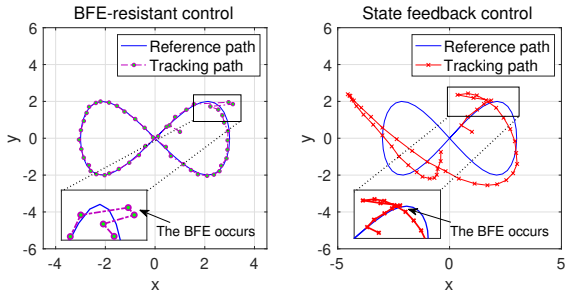

Fig. 2: Trajectory tracking performance under BFE-resistant control (left) and state feedback control (right) algorithms.

3) Chance constraints: In this subsection, we compare the method proposed in this paper with several other advanced approaches (e.g., [13], [32]) for solving chance-constrained problems. Before presenting the comparative results, we first set identical simulation conditions for all algorithms. In particular, the BFE issue occurs at the integer-bit positions of the transmitted signal during the time interval $3 \le t \le 5$. Figs. 3–6 present the results of 100 independent experiments under different control algorithms. Each figure includes the individual state trajectories from all runs, as well as the averaged state trajectory computed over the 100 experiments.

Specifically, Fig. 3 illustrates the state trajectories of the system under the control algorithm proposed in this paper. It can be observed that, despite the presence of BFE and stochastic noise, the system successfully satisfies both the chance constraints and mean-square bounded stability requirements. In contrast, Fig. 4 shows the state trajectories under conventional chance-constrained control algorithms (e.g., [13], [32]). Since existing methods do not account for the coupling between BFE and chance constraints, the resulting control inputs fail to stabilize the system, leading to divergence. To further demonstrate the effectiveness of the proposed chance-constrained control approach, we combine the aforementioned baseline methods with the BFE-resilient control algorithm and conduct comparative

simulations. The corresponding results are shown in Figs. 5–6. Although these combined methods successfully stabilize the system, they fail to satisfy the specified chance constraint performance. This results further confirm the advantage of the proposed algorithm in simultaneously addressing BFEs and ensuring chance constraint performance.

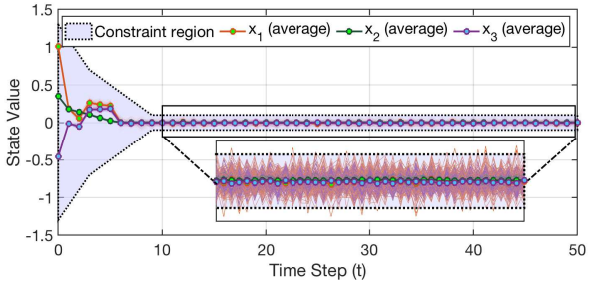

Fig. 3: State trajectories x_t based on the proposed chance-constrained BFE-resistant control algorithm.

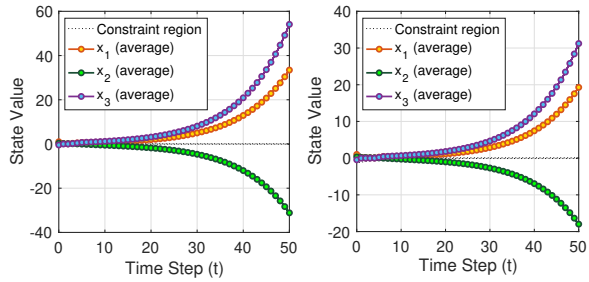

Fig. 4: State trajectories x_t based on the different existing chance-constrained control algorithms.

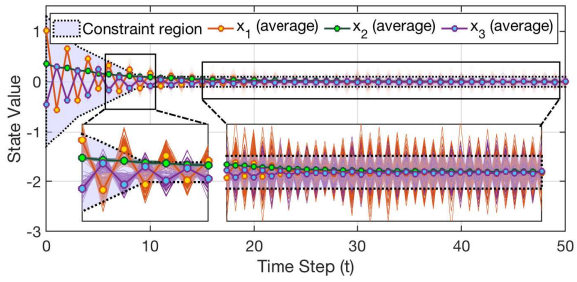

Fig. 5: State trajectories x_t under the chance-constrained solution proposed in [13] combined with the BFE-resistant control algorithm.

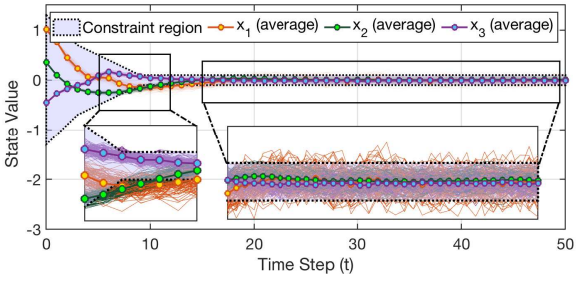

Fig. 6: State evolution x_t using the chance-constrained solution proposed in [32] combined with the BFE-resistant control algorithm.

4) Dynamic and static encoding mechanisms: To evaluate the effectiveness of the proposed DEM, we compare it against the conventional static encoding mechanism (SEM) (e.g., the method used in [19], [21]). Fig. 7 illustrates the amplitude changes of the control signals $\mathbf{Q}[u_t]$ under the SEM and $\hat{u}_t$ under the DEM. It is apparent that the amplitude of $\hat{u}_t$ consistently remains less than or equal to that of $\mathbf{Q}[u_t]$. This indicates that the DEM-based signal preprocessing method can effectively reduce communication burden during transmission over the network. Furthermore, 100 independent simulations are conducted under each encoding mechanism, and the corresponding average state trajectories are denoted by x_t^{avg}. Table I demonstrates that the control strategy based on DEM achieves improved control performance compared to the SEM-based control methods.

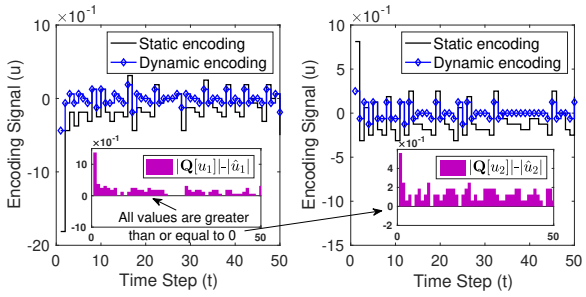

Fig. 7: Control input signals under the static and dynamic encoding mechanisms.

Encoding Mechanisms	DEM	SEM
$\sqrt{\frac{1}{50}\sum_{t=1}^{50}\|\|x_t^{\text{avg}}\|\|_2^2}$	0.2839	0.3128
$\|\|x_{50}^{\text{avg}}\|\|_2$	0.0693	0.1633

TABLE I: Control performance under different encoding mechanisms.

5) BFEs under various levels: In this subsection, we evaluate the control performance of the system under various BFE levels. Specifically, we consider the following three cases: 1) BFE occurs in the fractional-bit part of the transmitted signal within the time interval $6 \leq t \leq 8$; 2) BFE occurs in the integer-bit part of the transmitted signal within the same interval $6 \leq t \leq 8$; and 3) BFE affects the sign-bit of the transmitted signal over time intervals $6 \leq t \leq 8$ and $25 \leq t \leq 27$. Fig. 8 presents the system responses under these three BFE scenarios. It is evident that, despite differences in the location and duration of the BFEs, the system consistently maintains satisfactory control performance.

In summary, the above simulation results validate the effectiveness of the proposed algorithm.

V. Conclusion

In this investigation, the binary-encoding-based control issue has been addressed for uncertain systems with chance constraints and BFEs. A binary DEM has been proposed to alleviate the communication burden by encoding system data into a binary string with finite-length bits. The influence of the BFE phenomenon has been fully analyzed under the DEM-based control scheme. Subsequently, a novel BFE-resistant controller has been designed to counteract the coupling effects from the BFE and the DEM. A chance-constrained control scheme has then been constructed to ensure mean-square boundedness and adherence to the chance constraint index. A method for optimizing the controller parameters has been presented, and the simulation results have validated the reliability of the proposed control algorithm.

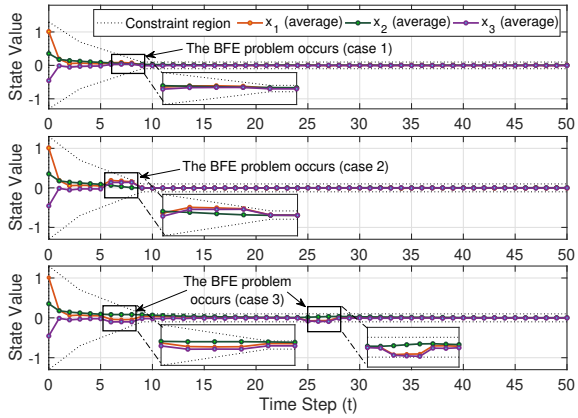

Fig. 8: State trajectories under different BFE levels.

REFERENCES

[1] A. Alessandri and M. Gaggero, Fast moving horizon state estimation for discrete-time systems with linear constraints, *International Journal of Adaptive Control and Signal Processing*, vol. 34, no. 6, pp. 706–720, 2020.

[2] A. Bernstein, K. Steiglita and J. Hopcroft, Encoding of analog signals for binary symmetric channels, *IEEE Transactions on Information Theory*, vol. 12, no. 4, pp. 425–430, 1966.

[3] S. A. Bowyer, B. L. Davies and F. R. y Baena, Active constraints/virtual fixtures: A survey, *IEEE Transactions on Robotics*, vol. 30, no. 1, pp. 138–157, 2014.

[4] R. Caballero-Águila, J. Hu and J. Linares-Pérez, Filtering and smoothing estimation algorithms from uncertain nonlinear observations with time-correlated additive noise and random deception attacks, *International Journal of Systems Science*, vol. 55, no. 10, pp. 2023–2035, 2024.

[5] A. Charnes and W. W. Cooper, Chance-constrained programming, *Management Science*, vol. 6, no. 1, pp. 73–79, 1959.

[6] C. Chen, W. Zou and Z. Xiang, Event-triggered consensus of multiple uncertain Euler-Lagrange systems with limited communication range, *IEEE Transactions on Systems, Man, Cybernetics: Systems*, vol. 53, no. 9, no. 5945–5954, 2023.

[7] J. Chen, C. Hua, S. Chen and C. Qian, Robust low-complexity vibration suppression control of rolling mill with time-varying state constraints, *International Journal of Systems Science*, vol. 56, no. 5, pp. 1081–1094, 2025.

[8] L. Dai, Y. Gao, L. Xie, K. H. Johansson and Y. Xia, Stochastic self-triggered model predictive control for linear systems with probabilistic constraints, *Automatica*, vol. 92, pp. 9–17, 2018.

[9] L. Dai, Y. Xia, Y. Gao and M. Cannon, Distributed stochastic MPC of linear systems with additive uncertainty and coupled probabilistic constraints, *IEEE Transactions on Automatic Control*, vol. 62, no. 7, pp. 3474–3481, 2016.

[10] N. Farvardin, A study of vector quantization for noisy channels, *IEEE Transactions on Information Theory*, vol. 36, no. 4, pp. 799–809, 1990.

[11] Y. Gao, L. Ma, M. Zhang, J. Guo and Y. Bo, Distributed set-membership filtering for nonlinear time-varying systems with dynamic coding-decoding communication protocol, *IEEE Systems Journal*, vol. 16, no. 2, pp. 2958–2967, 2022.

[12] J. Guanetti, Y. Kim and F. Borrelli, Control of connected and automated vehicles: State of the art and future challenges, *Annual Reviews in Control*, vol. 45, pp. 18–40, 2018.

[13] Y. Guo, Q. Liu, Z. Wang, Z. Zhang and X. He, Active fault diagnosis for linear stochastic systems subject to chance constraints, *Automatica*, vol. 156, 2024, Art. no. 111194.

[14] J. P. Hespanha, P. Naghshtabrizi and Y. Xu, A survey of recent results in networked control systems, *Proceedings of the IEEE*, vol. 95, no. 1, pp. 138–162, 2007.

[15] S. Hu, X. Ge, X. Chen and D. Yue, Resilient load frequency control of islander AC microgrids under concurrent false data injection and denial-of-service attacks, *IEEE Transactions on Smart Grid*, vol. 14, no. 1, pp. 690–700, 2023.

[16] Z. Hu, B. Chen, Z. Wang and L. Yu, Performance analysis of stochastic event-triggered estimator with compressed measurements, *Automatica*, vol. 162, 2024, Art. no. 111520.

[17] F. Jin, L. Ma, C. Zhao and Q. Liu, A quantization-coding scheme with variable data rates for cyber-physical systems under DoS attacks, *Systems Science & Control Engineering*, vol. 12, no. 1, 2024, Art. no. 2348690.

[18] C. Li, Y. Liu, M. Gao and L. Sheng, Fault-tolerant formation consensus control for time-varying multi-agent systems with stochastic communication protocol, *International Journal of Network Dynamics and Intelligence*, vol. 3, no. 1, 2024, Art. no. 100004.

[19] J. Li, H. Dong, Y. Shen and N. Hou, Encoding-decoding strategy based resilient state estimation for bias-corrupted stochastic nonlinear systems, *ISA Transactions*, vol. 127, pp. 80–87, 2022.

[20] J. Li, Y. Niu and D. W. C. Ho, Limited coding-length-based sliding-mode control with adaptive quantizer's parameter, *IEEE Transactions on Automatic Control*, vol. 67, no. 9, pp. 4738–4745, 2022.

[21] Q. Liu and Z. Wang, Moving-horizon estimation for linear dynamic networks with binary encoding schemes, *IEEE Transactions on Automatic Control*, vol. 66, no. 4, pp. 1763–1770, 2021.

[22] X. Lv, Y. Niu and Z. Cao, Sliding mode control for uncertain 2-D FMII systems under stochastic scheduling, *IEEE Transactions on Cybernetics*, vol. 54, no. 4, pp. 2554–2565, 2024.

[23] B. L. Miller and H. M. Wagner, Chance constrained programming with joint constraints, *Operations Research*, vol. 13, no. 6, pp. 930–945, 1965.

[24] C. R. Murthy and B. D. Rao, High-rate analysis of source coding for symmetric error channels, in: *Proceedings of the Data Compression Conference*, pp. 163–172, 2006.

[25] D. Pan, String stable bidirectional platooning control for heterogeneous connected automated vehicles, *International Journal of Network Dynamics and Intelligence*, vol. 3, no. 4, 2024, Art. no. 100026.

[26] F. Qu, E. Tian and X. Zhao, Chance-constrained H_∞ state estimation for recursive neural networks under deception attacks and energy constraints: The finite-horizon case, *IEEE Transactions on Neural Networks and Learning Systems*, vol. 34, no. 9, pp. 6492–6503, 2023.

[27] T. Shi and Z. Xiang, Asymptotic tracking control for a class of uncertain nonlinear systems with output constraint, *Applied Mathematics and Computation*, vol. 478, 2024, Art. no. 128845.

[28] J. Sun, B. Shen, Y. Liu and F. E. Alsaadi, Dynamic event-triggered state estimation for time-delayed spatial-temporal networks under encoding-decoding scheme, *Neurocomputing*, vol. 500, pp. 868–876, 2022.

[29] J. Vlassenbroeck, A Chebyshev polynomial method for optimal control with state constraints, *Automatica*, vol. 24, no. 4, pp. 499–506, 1988.

[30] X. Wan, C. Zhang, F. Wei, C.-K. Zhang and M. Wu, Hybrid dynamic variables-dependent event-triggered fuzzy model predictive control, *IEEE/CAA Journal of Automatica Sinica*, vol. 11, no. 3, pp. 723–733, 2024.

[31] W. Wang, L. Ma, Q. Rui and C. Gao, A survey on privacy-preserving control and filtering of networked control systems, *International Journal of Systems Science*, vol. 55, no. 11, pp. 2269–2288, 2024.

[32] B. Wei, E. Tian, T. Zhang and X. Zhao, Probabilistic-constrained H_∞ tracking control for a class of stochastic nonlinear systems subject to DoS attacks and measurement outliers, *IEEE Transactions on Circuits and Systems I: Regular Papers*, vol. 68, no. 10, pp. 4381–4392, 2021.

[33] Y. Xia, Cloud control systems, *IEEE/CAA Journal of Automatica Sinica*, vol. 2, no. 2, pp. 134–142, 2015.

[34] W. Yang, D. Li, H. Zhang, Y. Tang and W. X. Zheng, An encoding mechanism for secrecy of remote state estimation, *Automatica*, vol. 120, 2020, Art. no. 109116.

[35] X. Yi, H. Yu, Z. Fang and L. Ma, Probability-guaranteed state estimation for nonlinear delayed systems under mixed attacks, *International Journal of Systems Science*, vol. 54, no. 9, pp. 2059-2071, 2023.

[36] R. Zhang, H. Liu, Y. Liu and H. Tan, Dynamic event-triggered state estimation for discrete-time delayed switched neural networks with constrained bit rate, *Systems Science & Control Engineering*, vol. 12, no. 1, 2024, Art. no. 2334304.

[37] K. Zhu, Z. Wang, Y. Chen and G. Wei, Event-triggered cost-guaranteed control for linear repetitive processes under probabilistic constraints, *IEEE Transactions on Automatic Control*, vol. 68, no. 1, pp. 424–431, 2023.

[38] K. Zhu, Z. Wang, Y. Chen and G. Wei, Neural-network-based set-membership fault estimation for 2-D systems under encoding-decoding mechanism, *IEEE Transactions on Neural Networks and Learning Systems*, vol. 34, no. 2, pp. 786–798, 2023.